Rectangular and Annular Modal Analyses of Multimode Waveguide Bends

EZEKIEL BAHAR, SENIOR MEMBER, IEEE, AND GOPALAN GOVINDARAJAN, MEMBER, IEEE

Abstract—**Spurious modes in multimode *H*-plane waveguide bends of nonuniform curvature are computed on the basis of rectangular and annular waveguide modal analyses. The sets of coupled differential equations for the wave amplitudes are solved numerically using both an iterative approach and the Runge–Kutta method. The advantages and limitations of the different approaches to this problem are considered in detail.**

I. Introduction

WAVEGUIDE BENDS capable of supporting several propagating modes are of considerable practical importance in the design of high-powered microwave systems [1]. Several methods have been developed for the analysis of waveguide bends [2]–[4]. These methods result in the conversion of Maxwell's equations into infinite sets of coupled transmission-line equations referred to as "generalized telegraphist's equations." The dependent variables in these first-order coupled differential equations are the forward and backward waveguide mode amplitudes.

For the purpose of the analysis it is necessary to express the transverse components of the electric and magnetic fields at any cross section of the nonuniform waveguide in terms of a complete modal expansion. For the case of waveguide bends of rectangular cross section, it is possible to express the fields at any cross section, normal to the center line of the waveguide, in terms of local rectangular waveguide modes or in terms of local annular waveguide modes [4].

The solutions for the electromagnetic (EM) fields at any cross section do not depend on the particular modal expansion used. However, the sets of coupled differential equations for the wave amplitudes depend upon the modal expansion used in the analysis. Thus the solutions for the mode amplitudes, based upon the rectangular and annular modal analyses, are different except at bend cross sections where the center line radius of curvature is infinite and the two modal expansions merge.

The modal equation for rectangular waveguides can be readily solved. However, the modal equation for annular waveguides, which involves Bessel functions, needs to be solved numerically with the aid of a digital computer. Although it is easier to compute the coupling coefficients derived using the rectangular modal analysis, it is shown that when operating over a wide range of waveguide bend parameters, the analysis based on the annular modal expansion is more efficient.

The basic reasons for this are twofold. First, using the local annular modal analysis, the coupling into the spurious modes along the length of the waveguide bend is smaller. This permits the use of simple iterative approaches to the solution of the coupled differential equations over a much wider range of waveguide bend parameters when the annular modal analysis is used. Secondly, when the annular modal analysis is used, the significant spurious modes are bunched more tightly about the incident mode. As a result, fewer spurious modes need to be considered.

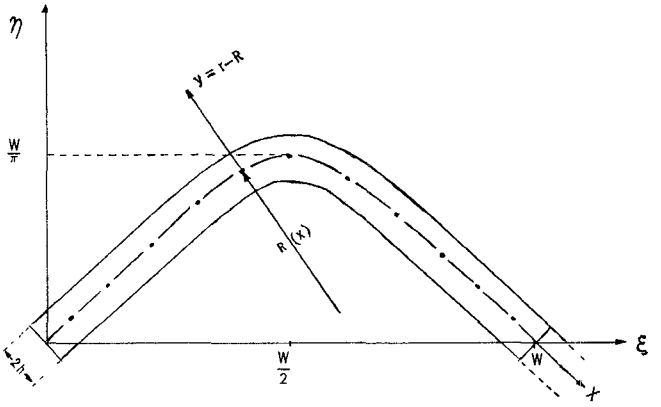

Fig. 1. *H*-plane waveguide bend with sinusoidally shaped center line.

H-plane waveguide bends with sinusoidally shaped center lines and uniform rectangular cross sections are considered in this paper in detail, in order to illustrate the advantages and the limitations of the different approaches to this problem. The numerical results obtained from two independent approaches to these problems provide a valuable means to check out the results before a model is constructed.

II. Formulation of the Problem

The center lines of the *H*-plane bends considered in this paper are given by the expression

$$\eta(\xi) = (w/\pi) \sin (\pi\xi/w), \qquad 0 \leq \xi \leq w \qquad (1)$$

where ξ is measured along the straight lines connecting the input and output ports of the waveguide bends (see Fig. 1), and w is one of the design parameters. Equation (1) describes 90° bends with infinite radii of curvature at the input and output ports. The uniform rectangular cross sections of the bends are $2h \times d$. The bends are assumed to be excited by $TE_{m,0}$ modes only. For *H*-plane bends the $TE_{m,0}$ modes couple with the $TE_{n,0}$ modes only ($m, n = 1, 2, 3, \cdots$) [4]. Thus the design parameter $2h$ (width of the cross section) determines the number of propagating modes that may be excited in the bend. Since mode coupling is independent of the parameter d (height of the cross section), d is left unspecified.

At any cross section of the waveguide bend the transverse components of the EM fields can be expressed in terms of

Manuscript received May 11, 1973; revised July 23, 1973. This work was supported in part by the National Science Foundation, and in part by the Engineering Research Center, University of Nebraska, Lincoln, Nebr.

The authors are with the Department of Electrical Engineering, University of Nebraska, Lincoln, Nebr. 68508.

complete rectangular or annular modal expansions. Thus E_z and H_y (see Fig. 1) are expressed as follows in terms of the forward and backward wave amplitudes a_n and b_n, respectively:

$$E_z = (a_n + b_n)\psi_n \qquad H_y = Y_n(a_n - b_n)\psi_n. \tag{2}$$

For the rectangular modes the basis functions are

$$\psi_n(y) = \sin\left[k_n(y+h)\right]/(Y_n h)^{1/2}, \qquad -h \le y \le h \tag{3a}$$

and for the annular modes they are given in terms of Hankel functions:

$$\psi_n(r) = A_n\left[H_{\nu n}^{(1)}(kr)H_{\nu n}^{(2)}(ka) - H_{\nu n}^{(1)}(ka)H_{\nu n}^{(2)}(kr)\right], \qquad a \le r \le b \tag{3b}$$

in which $a = R-h$, $b = R+h$, k is the free-space wavenumber, and R is the local radius of curvature of the center line. The constant A_n is

$$A_n = \frac{\pi k}{4i}\left(\frac{R_a C_n(R(C_n(a)}{hY_{nR}}\right)^{1/2}$$
$$C_n(r) = \left[1 - (\nu_n^2 - 1/4)/(kr)^2\right]^{1/2}. \tag{3c}$$

The modal equation for the rectangular modes is $\psi_n(h) = 0$; thus $k_n = n\pi/2h$. The modal equation for annular modes $\psi_n(b) = 0$ is solved numerically for the values of the mode numbers ν_n. The propagation coefficients (along the center line) are $\beta_n = (k^2 - k_n^2)^{1/2}$ and $\beta_n = \nu_n/R$ for the rectangular and annular modes, respectively. The nth-mode wave admittances for rectangular and annular modes are $Y_n = Y\beta_n/k$ and $Y_n = Y\beta_n R/kr \equiv Y_{nR}R/r$, in which Y is the free-space wave admittance.

The coupled differential equations for the wave amplitudes are

$$\frac{-da_n}{dx} - i\beta_n a_n = \sum_{m=1}^{\infty}\left(\frac{dS_{nm}^{BA}}{dx}a_m + \frac{dS_{nm}^{BB}}{dx}b_m\right) \tag{4a}$$

$$\frac{-db_n}{dx} + i\beta_n b_n = \sum_{m=1}^{\infty}\left(\frac{dS_{nm}^{AB}}{dx}b_m + \frac{dS_{nm}^{AA}}{dx}a_m\right) \tag{4b}$$

in which x is the distance measured along the center line of the bend. The transmission scattering (coupling) coefficients for the rectangular modes vanish for $n-m$ even. For $n-m$ odd they are

$$\frac{dS_{nm}^{AB}}{dx} = \frac{dS_{nm}^{BA}}{dx} = \frac{-i4nm(\beta_n\beta_m)^{-1/2}}{(n^2-m^2)^2\pi^2}\left(\frac{h}{R}\right) \cdot(\beta_n + \beta_m)^2. \tag{5a}$$

For the annular modes they are for $n-m$ both even and odd

$$\frac{dS_{nm}^{AB}}{dx} = \frac{dS_{nm}^{BA}}{dx} = \frac{1}{2}(C_{nm} - C_{mn}) \tag{5b}$$

$$C_{nm} = \frac{Y_{nR}kR}{(\nu_n^2 - \nu_m^2)}\frac{\nu_n^2 + 3\nu_m^2 - 1}{\left[\nu_n^2 - (\nu_m+1)^2\right]\left[\nu_n^2 - (\nu_m - 1)^2\right]} \cdot\left[kr\psi_n'\psi_m'\right]_a^b\frac{dR}{dx}, \qquad n \neq m. \tag{5c}$$

In the following section we derive numerical solutions to (4) for both the rectangular and annular modal analyses. Since the basis functions for both analyses merge at the input and output ports of the bend, the mode amplitudes at these ports must also be the same in order to satisfy (2). It is interesting to point out that even though the coupling coefficients for the rectangular modes vanish when $m-n$ is even, any given incident mode will excite both even and odd numbered modes [4].

III. Illustrative Examples

The radius of curvature $R(\xi)$ of the bend center line defined by $\eta(\xi)$, (1), is minimum at the center where

$$R_{\min} = \left[1 + (\eta')^2\right]^{3/2}/\eta'' = w/\pi \tag{6a}$$

and the primes denote differentiation with respect to ξ. In this work we have considered two cross-section widths

$$2h/\lambda = 1.75 \quad \text{and} \quad 2h/\lambda = 2. \tag{6b}$$

The minimum value for w considered is $w/2h = 6$; thus at any cross section of the bend, $\lambda/R < 0.3$. In Fig. 2(a) and (b) the values of β_n/k $(n = 1, 2, 3)$ are plotted as functions of λ/R for the annular modes. The values for β_n/k for rectangular waveguides can be obtained from these figures by setting $\lambda/R = 0$. It is interesting to note that for small center line radii of curvature bends, the dominant annular mode $(n = 1)$ becomes a slow wave (the phase velocity is smaller than the free-space velocity of the wave $\beta_1/k > 1$). This corresponds to the well-known phenomenon of the earth detached modes in the earth–ionosphere waveguide [5], [6].

Since the radius of curvature (6a) is an explicit function of ξ rather than x (the distance along the center line), it is simpler to express the wave amplitudes as functions of ξ. To this end we multiply (4) by $dx/d\xi$, where

$$\frac{dx}{d\xi} = (1 + (\eta')^2)^{1/2}. \tag{7}$$

When the power coupled into the spurious modes at any cross section of the bend is small, a simple iterative approach may be used to solve (4) for the wave amplitudes.

Thus for the mth incident mode we get the Wentzel–Kramers–Brillouin- (WKB) type solution

$$a_m(\xi) = a_m(0)\exp\left\{-i\int_0^{\xi}\left(\beta_m\frac{dx}{d\xi^*}\right)d\xi^*\right\}. \tag{8a}$$

The spurious mode wave amplitudes are

$$a_n(\xi) = -a_m(0)\exp\left\{-i\int_0^{\xi}\left(\beta_n\frac{dx}{d\xi^*}d\xi^*\right\}\right.\int_0^{\xi} \cdot\exp\left\{-i\int_0^{\xi^*}(\beta_m - \beta_n)\frac{dx}{d\xi}d\xi\right\}\frac{dS_{nm}^{BA}}{dx}\frac{dx}{d\xi^*}d\xi^*. \tag{8b}$$

In addition to the above iterative solutions, the coupled differential equations have also been solved numerically using a fifth-order Runge–Kutta method. Here we have neglected reflections $(b_n = 0)$, and assumed that the incident mode corresponds to $m = 1$ and the spurious modes are $n = 2$ and 3. For convenience we set $a_1(0) = 1$. In Fig. 3(a) and (b), the Runge–Kutta solutions for $|a_1(\xi)|$ are plotted as functions of ξ/w for $w/2h = 14$ and $w/2h = 6$, respectively, with $2h/\lambda = 1.75$. The solutions are given for the rectangular and annular modal analyses. The corresponding iterative solutions are $|a_1(\xi)| = 1$. Clearly, the rectangular and annular modal analyses are in

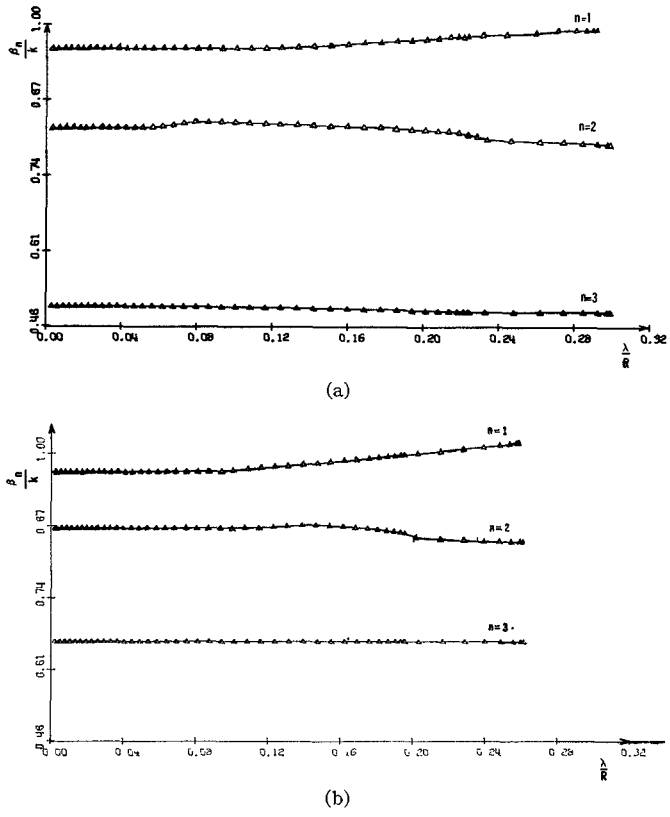

Fig. 2. Propagation coefficient for annular modes β_n. (a) $2h/\lambda = 1.75$. (b) $2h/\lambda = 2.0$.

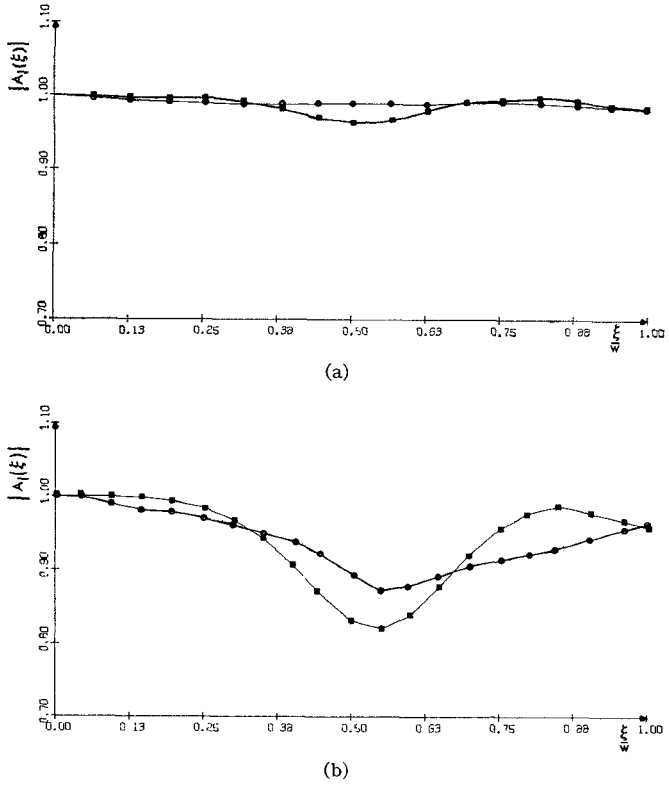

Fig. 3. Amplitude of incident mode $|a_1(\xi)| = |A_1(\xi)|$; $2h/\lambda = 1.75$. (a) $w/2h = 14$. (b) $w/2h = 6$; Runge–Kutta solutions. ■ Rectangular. ○ Annular.

good agreement for $\xi = w$; however, $|a_1(\xi)|_{\min}$ is smaller when the rectangular modal analysis is used due to stronger mode coupling.

In Fig. 4(a) and (b), $|a_2(\xi)|$ is plotted as a function of ξ/w for $w/2h = 14$ and $w/2h = 6$, respectively. Similarly, in Fig. 5(a) and (b), $|a_3(\xi)|$ is plotted for $w/2h = 14$ and $w/2h = 6$. For all these plots, $2h/\lambda = 1.75$. In Fig. 4 both the iterative and the Runge–Kutta solutions are provided for the rectangular as well as the annular modal analyses.

For $w/2h = 14$, [Fig. 4(a)] the iterative solutions are in good agreement with the Runge–Kutta solution (especially when the annular modal analysis is used). As pointed out in Section II, $|a_n(\xi)|$ depends on the particular modal analysis used, except at the ports of the waveguide bend where these values merge.

When $w/2h = 6$ [Fig. 4(b)], we find that the iterative solution is in good agreement with the Runge–Kutta solution only when the annular modal analysis is used. The iterative solution based on the rectangular modal analysis fails. This is due to the relatively large amount of power coupled into the spurious modes. From Fig. 5 it is clear that for $w/2h = 14$, the presence of the third mode could be entirely ignored when the annular modal analysis is used; thus only two modes need to be considered in solving (4). A similar comparison of $|a_3(\xi)|$ for $w/2h = 6$ (Fig. 5) shows that, in general, the maximum value of $|a_3(\xi)|$ is larger when the rectangular modal analysis is used. In Fig. 5 only the Runge–Kutta solutions are given.

In Fig. 6(a), $|a_2(w)|$ is plotted as a function of $w/2h$ for $2h/\lambda = 1.75$. Four plots are given—the iterative and Runge–Kutta solutions for both the rectangular and annular modal analysis. All four curves for $|a_2(w)|$ are in good agreement for $w/2h \geq 12$. The Runge–Kutta solution for the rectangular modal analysis is in agreement with both curves corresponding to the annular modal analysis, even for $w/2h < 12$. The iterative solution, however, is obviously incorrect for $w/2h < 12$ when the rectangular modal analysis is used. This is due to the large amount of power coupled into the spurious modes. In Fig. 6(b), $|a_2(w)|$ is plotted as a function of $w/2h$ for $2h/\lambda = 2$. Here the iterative and Runge–Kutta solutions using the annular modal analysis are given. Note that in this case when $|a_2(w)| > 0.3$, the iterative solution is not in agreement with the Runge–Kutta solution.

In order to enhance our physical understanding of the coupling phenomena, we study in detail the case $w/2h = 14$, $2h/\lambda = 1.75$. For clarity of presentation we define the expression for $A_n(\xi)$ as follows:

$$A_n(\xi) = a_n(\xi) \exp\left\{-i \int_{\xi}^{w} \beta_n \frac{dx}{d\xi^*}\right\}. \tag{9a}$$

Thus $A_n(w) = a_n(w)$, and $|A_n(\xi)| = |a_n(\xi)|$. The phasor

$$\Delta A_2 = A_2(\xi + \Delta\xi) - A_2(\xi) \tag{9b}$$

represents the contribution to the spurious mode $a_2(w)$ from the element of the waveguide bend that lies between ξ and $\xi + \Delta\xi$. In Fig. 7(a) and (b), respectively, we have plotted the iterative and Runge–Kutta solutions for $A_2(\xi)$ using the rectangular modal analysis. In Fig. 8(a) and (b), respectively, we have plotted the iterative and Runge–Kutta solutions for $A_2(\xi)$ based on the annular modal analysis. At the origin, $\xi = 0$, and at the end of the curve, $\xi = w$. $A_2(\xi)$ is the line that joins the origin to any point on the curve. Clearly, the values of $A_2(w)$ [and $a_2(w)$] are in good agreement on all four curves

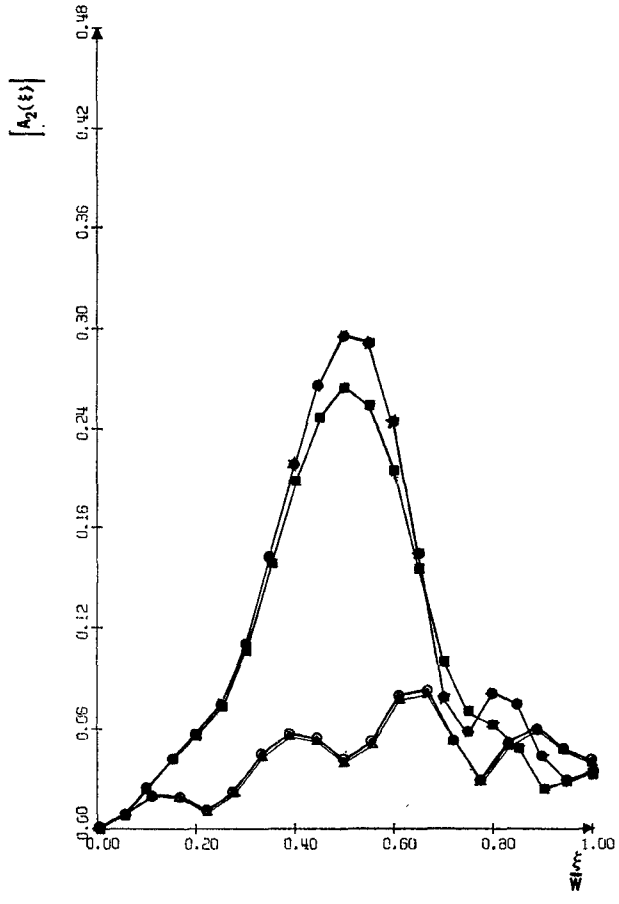

(a)

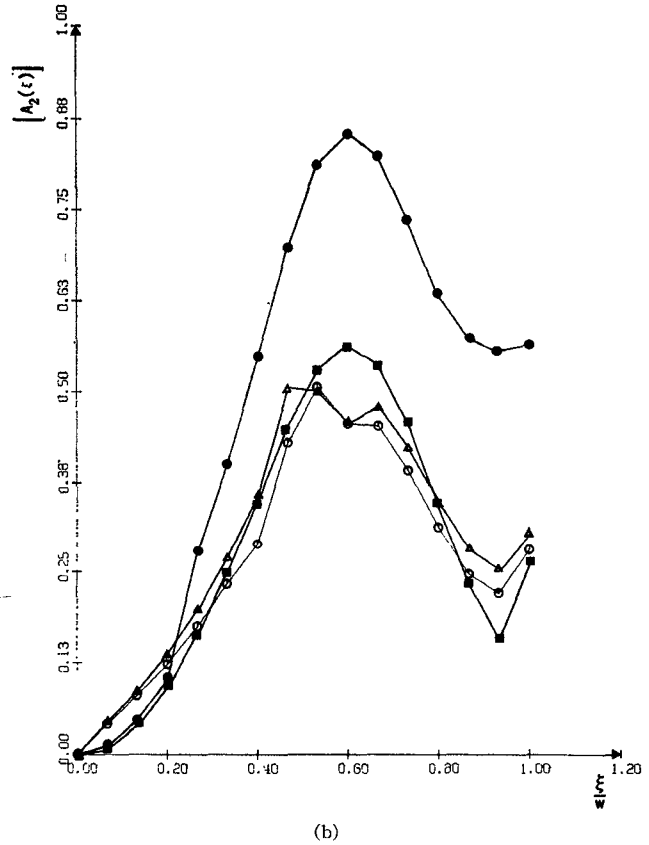

(b)

Fig. 4. Amplitude of spurious mode $|a_2(\xi)| = |A_2(\xi)|$; $2h/\lambda = 1.75$. (a) $w/2h = 14$. (b) $w/2h = 6$. ● Rectangular; iterative. ■ Rectangular; Runge–Kutta. △ Annular; iterative. ○ Annular; Runge–Kutta.

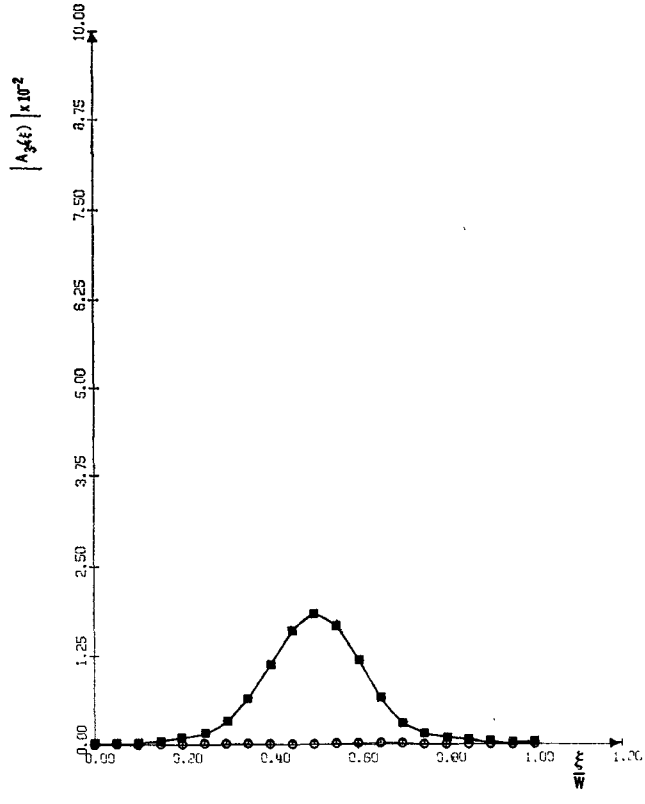

(a)

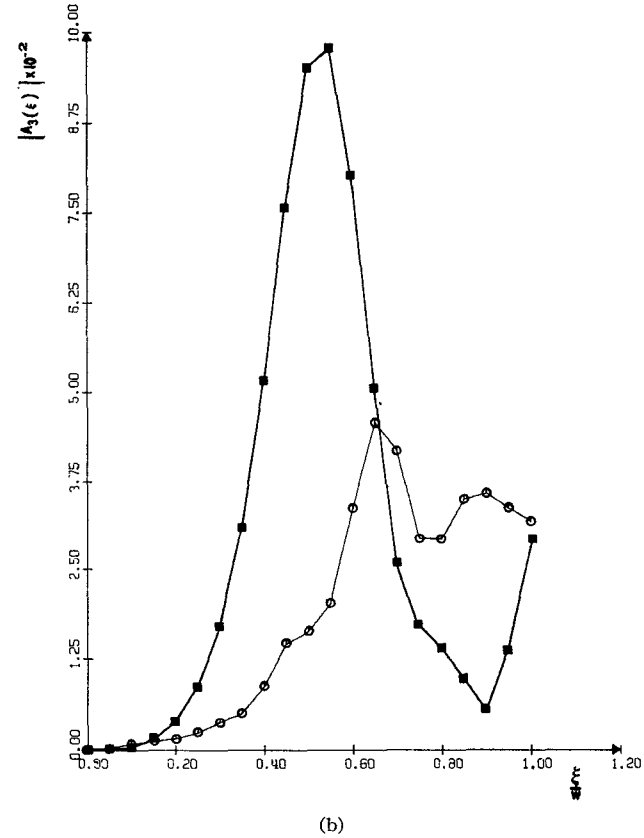

(b)

Fig. 5. Amplitude of spurious mode $|a_3(\xi)| = |A_3(\xi)|$; $2h/\lambda = 1.75$. (a) $w/2h = 14$. (b) $w/2h = 6$; Runge–Kutta solutions. ■ Rectangular. ○ Annular.

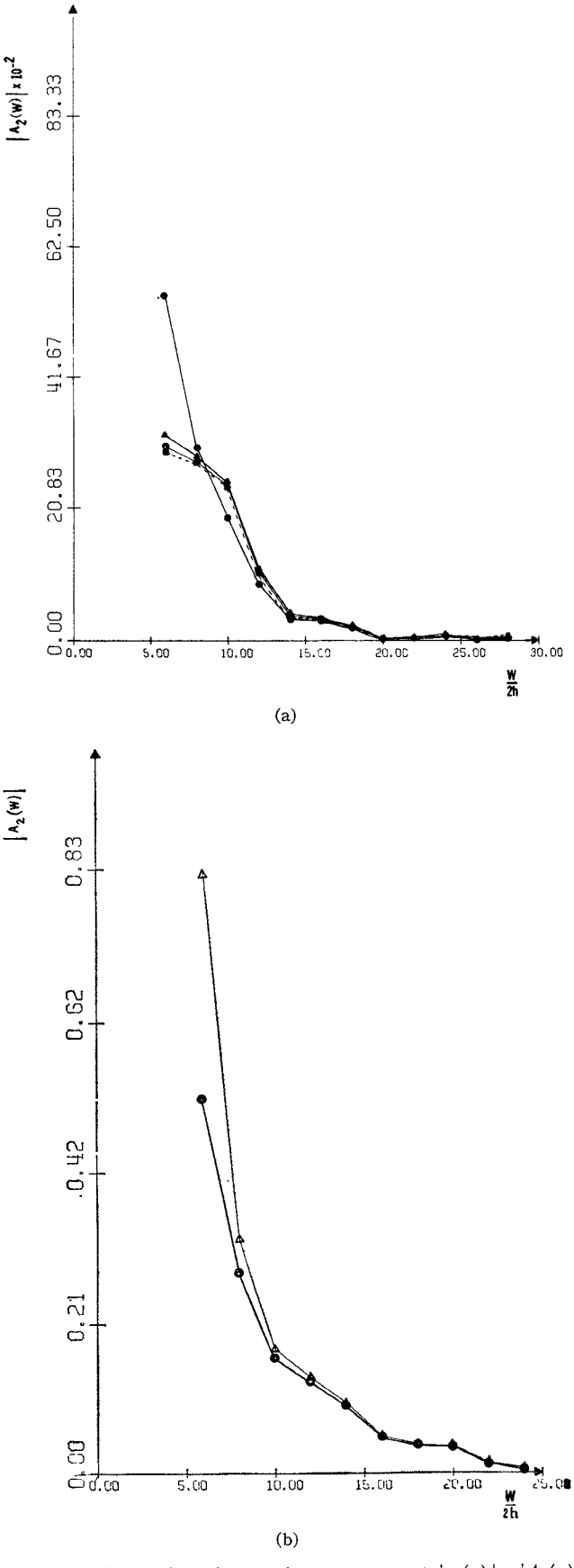

Fig. 6. Amplitude of spurious mode at output port $|a_2(w)| = |A_2(w)|$. (a) $2h/\lambda = 1.75$. (b) $2h/\lambda = 2.0$. ● Rectangular; iterative. ■ Rectangular; Runge–Kutta. △ Annular; iterative. ○ Annular; Runge–Kutta.

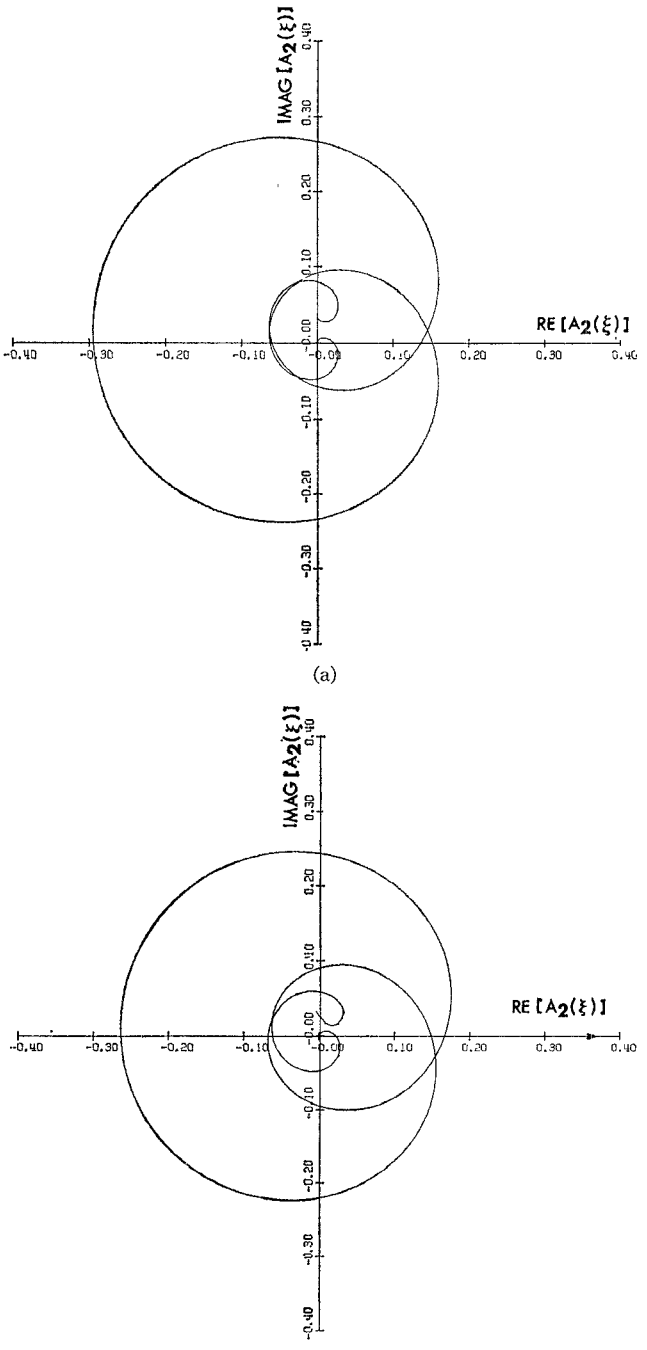

Fig. 7. Phasor diagram for $A_2(\xi)$ (3.5a). Rectangular modal analysis. (a) Iterative solution. (b) Runge–Kutta solution.

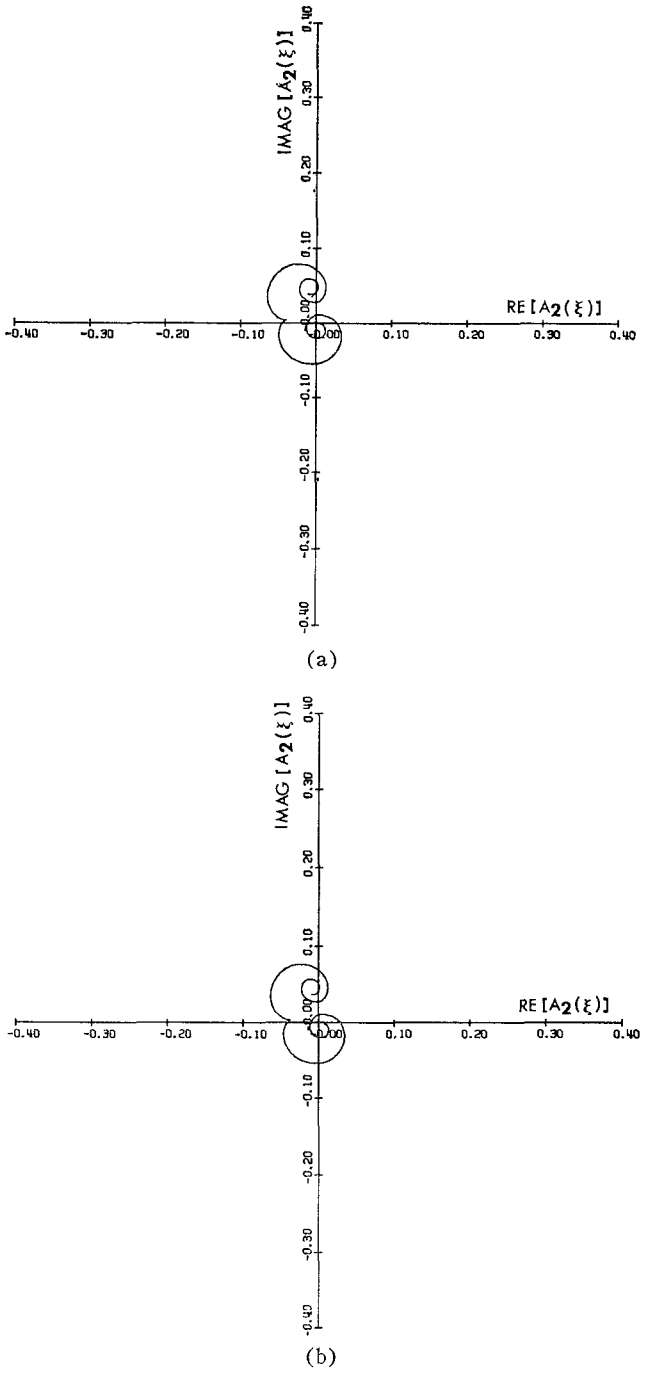

Fig. 8. Phasor diagram for $A_2(\xi)$ (3.5a). Annular modal analysis. (a) Iterative solution. (b) Runge–Kutta solution.

(Figs. 7 and 8). However, $|A_2(\xi)|_{\max}$ is much larger when the rectangular modal analysis is used. Using the annular modal analysis (Fig. 8), $|A_2(\xi)|_{\max} < 0.1$. Thus less than 1 percent of the incident power is coupled into the spurious mode at any cross section of the bend. As a result, the iterative solution [Fig. 8(a)] is hardly distinguishable from the Runge–Kutta solution [Fig. 8(b)]. On the other hand, when the rectangular modal analysis is used, $|A_3(\xi)|_{\max} \approx 0.3$. Thus near the center of the bend about 10 percent of the incident power is coupled into the spurious mode. We see that the largest discrepancies between the iterative and Runge–Kutta solutions lie near the center of the bend where the spurious mode amplitude is largest.

Since $d\eta/d\xi$ and $d^3\eta/d\xi^3$ vanish at $\xi = w/2$, the coupling coefficient C_{nm} (5c) changes its sign at $\xi = w/2$. This is reflected as an abrupt change in the direction of the curve $A_2(\xi)$ at the center of the bend.

IV. Concluding Remarks

The design of multimode H-plane bends is considered in detail using two distinct analytical approaches to the problem. The coupled differential equations obtained from the rectangular and annular modal analysis are solved numerically using both an iterative method as well as the Runge–Kutta method.

To obtain the iterative solutions, the computer time required is about the same whether the rectangular or annular modal analysis is used. However, the range of the design parameters for which the iterative solution is valid depends on the maximum power coupled into the spurious modes. Hence, the iterative solutions are generally valid over a wider range of the design parameters when the annular modal analysis is used.

The Runge–Kutta solution based on the annular modal analysis took about five times longer to execute when compared with the corresponding iterative solution. On the other hand, the Runge–Kutta solution based on the rectangular modal analysis took about eight times longer to execute when compared with the corresponding iterative solution. When the annular modal analysis is used, the maximum spurious mode amplitudes are smaller; thus fewer spurious modes need to be considered in order to solve the coupled differential equations for the wave amplitudes (4).

The need to suppress spurious modes is a principal factor to be considered when waveguide bends are designed. Thus for a 90° waveguide bend with a sinusoidally shaped center line (1), corresponding to $w/2h = 14$ and $2h/\lambda = 1.75$, $20 \log |a_2(L)/a_1(L)| = 30$. Since in this case, the spurious mode amplitude is 30 dB below the principal mode amplitude, mode filters are not needed to suppress the spurious modes. Furthermore, Fig. 6(a) shows that any increase in the size of the waveguide bend does not significantly improve its performance. The programs used to compute the numerical data in this paper will be available from the authors upon request.

Acknowledgment

The authors wish to thank A. R. Edison and L. Lipsky for their comments, L. Berry for providing a subroutine for evaluating Bessel functions, and Mrs. E. Everett for typing the manuscript.

References

[1] J. P. Quine, "E- and H-plane bends for high-power oversized rectangular waveguide," *IEEE Trans. Microwave Theory Tech. (1964 Symposium Issue)*, vol. MTT-13, pp. 54–36, Jan. 1965.
[2] S. A. Schelkunoff, "Generalized telegraphist's equations for waveguides," *Bell Syst. Tech. J.*, vol. 31, pp. 784–801, July 1952.
[3] H. Zucker and G. I. Cohn, "Propagation of TE modes in nonuniform waveguides," *IRE Trans. Microwave Theory Tech.*, vol. MTT-10, pp. 202–208, May 1962.
[4] E. Bahar, "Fields in waveguide bends expressed in terms of coupled local annular waveguide modes," *IEEE Trans. Microwave Theory Tech.*, vol. MTT-17, pp. 210–217, Apr. 1969.
[5] J. R. Wait, "On the propagation of VLF and ELF radio waves when the ionosphere is not sharply bounded," *J. Res. Nat. Bur. Stand.*, sect. 68D, pp. 81–94, 1964.
[6] E. Bahar, "Computations of mode-scattering coefficients due to ionospheric perturbations and comparison with VLF radio measurements," *Proc. Inst. Elec. Eng.*, vol. 117, pp. 735–738, Apr. 1970.